Electronic Supplementary Material (ESI) for Energy & Environmental Science.

Supporting Information

Scalability and feasibility of photoelectrochemical H_2 evolution: The ultimate limit of Pt nanoparticle as an HER catalyst

E. Kemppainen, A. Bodin, B. Sebok, T. Pedersen, B. Seger, B. Mei, D. Bae, P. C. K. Vesborg, J. Halme, O. Hansen, P.D. Lund and I. Chorkendorff

We provide here the theoretical background and computational details of our model, as well as selected results that are helpful for understanding the details of reaction kinetics and mass transport in the model. The details of the model may not be interesting for the general readership, but for those interested in the topic, we provide here the details of what is modeled, and how that is done mathematically. Additionally, XPS analysis of deposited Pt loadings is provided.

Theory

Coupled mass transport and kinetic model of HER on Pt

The voltage losses of an electrode consist of mass transport and reaction kinetics. Because mass transport losses correspond to concentration changes at the vicinity of the electrode surface, they affect the reaction kinetics and for an accurate description of a reaction both processes have to be considered together as a coupled system. In this section we describe first the general implications of mass transport on HER (and HOR) overpotential, and thereafter our HER model, starting from reaction kinetics and continuing with mass transport in electrolyte. The description includes not only the final equations of the model, but also the derivation of some of them in order to clarify their physical basis. The purpose of this section is to explain our general understanding of HER/HOR on Pt and then describe the used model in enough detail that interested readers can reproduce it on their own.

Model of HER reaction kinetics on Pt

HER and HOR on platinum (Pt) are among the most studied reactions in electrochemistry. Despite that, the exact reaction mechanism and the exchange current density are current research topics[1,2]. For characterization studies acids are more problematic than alkaline electrolytes, because the kinetics are significantly faster, meaning that e.g. rotating disc electrodes (RDE) do not allow high enough mass transport rates to enable reliable estimation of reaction kinetics[1,3,4]. The total reaction in acid is

$$2\,H^+ + 2e^- \rightleftarrows H_2 \qquad \text{(S1)}$$

HER/HOR can proceed via the Volmer, Heyrovsky and Tafel reaction steps. In acid these reactions are:
Volmer

$$H^+ + e^- \rightleftarrows H_{ad} \qquad \text{(S2a)}$$

Heyrovsky

$$H^+ + e^- + H_{ad} \rightleftarrows H_2 \qquad \text{(S2b)}$$

Tafel

$$2H_{ad} \rightleftarrows H_2 \qquad \text{(S2c)}$$

The total reaction is typically considered to proceed through Volmer-Tafel or Volmer-Heyrovsky paths[1,3,5] and recent results indicate Volmer-Tafel path, with Volmer as the rate limiting step (RLS) [1,2,6].
The exchange current density of HER on Pt in acid is known to be high, but the exact value is debated. Values up to 600 mA/cm^2 have been reported[3], and although the exact value depends on temperature, at room temperature it appears to be at least about 100 mA/cm^2 [6]. However, it is more common to encounter significantly lower values (in the order of 0.1 – 10 mA/cm^2) together with Tafel step as the RLS, in contrast to Volmer as the RLS with recently reported high exchange current densities[3,6]. A likely explanation is that the low exchange current densities correspond to mass transport limitation of HOR, which produces an overpotential that resembles the kinetic overpotential when Tafel step is the RLS (details in next section)[2,6,7].

We use the dual-pathway kinetic model derived by Wang et al.[5] as a basis to derive expressions for HER/HOR that rigorously consider the concentrations of protons and H_2 as well as the fraction of reaction sites on Pt covered with adsorbed hydrogen atoms. We assume that the reaction proceeds via Volmer-Tafel path with Volmer step as the RLS. The total current density is then given by the Volmer rate (v_V, i_V), as the Heyrovsky rate is assumed to be zero and no electrons are involved in Tafel reaction (v_T). However the Tafel reaction affects the Volmer rate and overpotential via the fraction of reaction sites covered by adsorbed hydrogen (θ).

It is commonly accepted that the symmetry factor of Heyrovsky and Volmer reactions is ½. The net rate of each step is the difference of the forward (HOR) and backward (HER) rates:

$$v_T = k_T(1-\theta)^2 C_{H_2} - k_{-T}\theta^2 \tag{S3a}$$

$$v_H = k_H(1-\theta)C_{H_2} e^{{q_eV}/{2k_BT}} - k_{-H}\theta C_{H^+} e^{{-q_eV}/{2k_BT}} \tag{S3b}$$

$$v_V = k_V\theta e^{{q_eV}/{2k_BT}} - k_{-V}(1-\theta)C_{H^+} e^{{-q_eV}/{2k_BT}} \tag{S3c}$$

The *k*s represent the rate constant of the reactions, those with '-' in their subscript correspond to the reverse reaction (i.e. HER) and C_{H2} and C_{H^+} are the concentrations of hydrogen molecules and protons. The voltage *V* is the electrode potential minus the electrostatic potential in electrolyte, i.e. $V_s - V_l$ in the notation used later. When the electrode is at the reversible potential (V_0), the net current is zero and all forward rates are equal to the respective backward rates, so the exchange rates for the reactions can be expressed as

$$v_{0T} = k_T(1-\theta^0)^2 C_{H_2}^0 = k_{-T}(\theta^0)^2 \tag{S4a}$$

$$v_{0H} = k_H(1-\theta^0)C_{H_2}^0 e^{\frac{q_eV_0}{2k_BT}} = k_{-H}\theta^0 C_{H^+}^0 e^{\frac{-q_eV_0}{2k_BT}} \tag{S4b}$$

$$v_{0V} = k_V\theta^0 e^{\frac{q_eV_0}{2k_BT}} = k_{-V}(1-\theta^0)C_{H^+}^0 e^{\frac{-q_eV_0}{2k_BT}} \tag{S4c}$$

Superscript 0 denotes a concentration or coverage at $V=V_0$. We denote the overpotential with

$$\eta_{sl} = \frac{q_e\left(V_s - (V_l + V_0)\right)}{k_BT} \tag{S5a}$$

where the potential of the electrode is V_s and V_0+V_l is the potential in the electrolyte, with V_0 corresponding to Nernst potential of the reaction with the bulk concentrations (i.e. 0 V vs. RHE). Potential V_l corresponds to voltage losses in the electrolyte (equation (S22)), but not to the total mass transport losses. Note that this difference is not the total overpotential of the simulated system, but the driving force of the reaction at catalyst surface. The total overpotential corresponds to V_s at the "bottom" of the TiO_2 substrate (z=-100 nm, see also equation (S26)), and V_s at Pt surface includes ohmic losses in TiO_2 and Pt. However, since these losses were negligible (less than 1 mV in all studied cases)

$$\eta_{total} = V_s(z = -100nm) \approx V_{s,Pt} \tag{S5b}$$

Dividing the reaction rates with their exchange rates yields

$$v_T = v_{0T}\left[\left(\frac{1-\theta}{1-\theta^0}\right)^2 \frac{C_{H_2}}{C_{H_2}^0} - \left(\frac{\theta}{\theta^0}\right)^2\right] \tag{S5c}$$

$$v_H = v_{0H}\left[\left(\frac{1-\theta}{1-\theta^0}\right)\frac{C_{H_2}}{C_{H_2}^0} e^{\frac{\eta_{sl}}{2}} - \frac{C_{H^+}\theta}{C_{H^+}^0\theta^0} e^{-\frac{\eta_{sl}}{2}}\right] \tag{S5d}$$

$$v_V = v_{0V}\left[\frac{\theta}{\theta^0}e^{\frac{\eta_{sl}}{2}} - \frac{C_{H^+}}{C_{H^+}^0}\left(\frac{1-\theta}{1-\theta^0}\right)e^{-\frac{\eta_{sl}}{2}}\right] \tag{S5e}$$

The total current density is then the sum of the Volmer and Heyrovsky rates (multiplied by the elementary charge and Avogadro number). Because we assume the Heyrovsky rate to be zero, the electric current corresponds to Volmer reaction.

$$i = i_V = q_e N_A v_{0V}\left[\frac{\theta}{\theta^0}e^{\frac{\eta_{sl}}{2}} - \frac{C_{H^+}}{C_{H^+}^0}\left(\frac{1-\theta}{1-\theta^0}\right)e^{-\frac{\eta_{sl}}{2}}\right] = i_{0V}\left[\frac{\theta}{\theta^0}e^{\frac{\eta_{sl}}{2}} - \frac{C_{H^+}}{C_{H^+}^0}\left(\frac{1-\theta}{1-\theta^0}\right)e^{-\frac{\eta_{sl}}{2}}\right] \tag{S6}$$

The main difference of our model to the original model of Wang et al. is that we do not neglect proton concentration, and therefore the resulting model can account for its effect on the HER/HOR kinetics.

Since we simulate the reaction in conditions that correspond to C_{H+}^0=1M and p_{H2}=1bar, the reference conditions correspond to Standard Hydrogen Electrode (or equivalently RHE at pH=0). Surface proton and H_2 concentrations are given by the mass transport model coupled with this model, but the hydrogen coverage (θ) needs to be solved. The equilibrium surface coverage of adsorbed H, θ^0, is assumed to be 0.67 based on the results of Markovic and Ross[8].

Wang et al. derived both an exact solution and an approximation for the coverage at potential range that corresponds to HOR. However, they assumed infinitely fast mass transport, so the concentrations were neglected. Taking the concentration-dependence of the reactions into account changes the exact solution a bit. In steady state the coverage does not change with respect to time

$$\frac{d\theta}{dt} = 2v_T + v_H - v_V = 0 \tag{S7}$$

Using the concentration-dependent expressions for the reaction rates (equation (S5)) we get

$$-2v_{0T}\left[\left(\frac{1-\theta}{1-\theta^0}\right)^2\frac{C_{H_2}}{C_{H_2}^0} - \left(\frac{\theta}{\theta^0}\right)^2\right] - v_{0H}\left[\left(\frac{1-\theta}{1-\theta^0}\right)\frac{C_{H_2}}{C_{H_2}^0}e^{\frac{\eta_{sl}}{2}} - \frac{C_{H^+}\,\theta}{C_{H^+}^0\,\theta^0}e^{-\frac{\eta_{sl}}{2}}\right] + v_{0V}\left[\frac{\theta}{\theta^0}e^{\frac{\eta_{sl}}{2}} - \frac{C_{H^+}}{C_{H^+}^0}\left(\frac{1-\theta}{1-\theta^0}\right)e^{-\frac{\eta_{sl}}{2}}\right] = 0 \tag{S8}$$

Defining the ratio of Tafel and Heyrovsky rates to the Volmer rate (r_T=v_{0T}/v_{0V}, r_H=v_{0H}/ v_{0V}) and y=θ/θ^0 similarly to Wang et al. we get

$$-2r_T\left[(1-\theta^0 y)^2\frac{C_{H_2}}{C_{H_2}^0} - (1-\theta^0)^2 y^2\right] - r_H(1-\theta^0)\left[(1-\theta^0 y)\frac{C_{H_2}}{C_{H_2}^0}e^{\frac{\eta_{sl}}{2}} - \frac{C_{H^+}}{C_{H^+}^0}(1-\theta^0)ye^{-\frac{\eta_{sl}}{2}}\right] + (1-\theta^0)^2 ye^{\frac{\eta_{sl}}{2}} - (1-\theta^0)$$
$$(1-\theta^0 y)\frac{C_{H^+}}{C_{H^+}^0}e^{-\frac{\eta_{sl}}{2}} = 0 \tag{S9}$$

This is then arranged to a quadratic equation that is solved for y=θ/θ^0.

$$Ay^2 + By + C = 0 \tag{S10a}$$

$$\theta = \theta^0 y = \theta^0\frac{-B + \sqrt{B^2 - 4AC}}{2A} \tag{S10b}$$

The positive root is chosen, because it yields y=1 at η=0 (when C_i=C_i^0 for both protons and H_2). The terms *A, B* and *C* are

$$A = 2r_T\left[(1-\theta^0)^2 - (\theta^0)^2\frac{C_{H_2}}{C_{H_2}^0}\right] \tag{S10c}$$

$$B = 4r_T\theta^0\frac{C_{H_2}}{C_{H_2}^0} + e^{\frac{\eta_{sl}}{2}}\left(1-\theta^0\right)\left[\left(r_H\frac{C_{H_2}}{C_{H_2}^0}\theta^0 + 1 - \theta^0\right)\right] + e^{-\frac{\eta_{sl}}{2}}\left(1-\theta^0\right)\frac{C_{H^+}}{C_{H^+}^0}\left[r_H\left(1-\theta^0\right)+\theta^0\right] \tag{S10d}$$

$$C = -2r_T\frac{C_{H_2}}{C_{H_2}^0} - r_H\left(1-\theta^0\right)\frac{C_{H_2}}{C_{H_2}^0}e^{\frac{\eta_{sl}}{2}} + \left(1-\theta^0\right)\frac{C_{H^+}}{C_{H^+}^0}e^{-\frac{\eta_{sl}}{2}} \tag{S10e}$$

We assumed Volmer-Tafel mechanism with Volmer as the rate limiting step as recent results indicate[2,6]. The rate of Heyrovsky reaction is assumed to be zero ($r_H = 0$), and the exchange current density of Volmer reaction (i_{0V}) 100 mA/cm^2, based on the recent results of Durst et al.[6]. The ratio of Tafel and Volmer exchange rates (r_T) is not known with certainty, but a range for the possible values can be estimated based on the kinetic limitations that Tafel-step imposes on the HER and HOR current densities. Only Tafel reaction produces H_2, but in steady state its rate is equal to the rate of Volmer reaction. Therefore current density (Volmer rate) yields the correct H_2 production rate, and it is sufficient to consider how Tafel rate affects the surface coverage (θ and r_T).

Mass transport overpotential of HER on Pt

With negligible kinetic losses (i.e. exchange current density is high compared to current density on catalyst) the electrode potential is equal to the Nernst potential of the electrolyte at its surface. The Nernst potential of the hydrogen electrode is:

$$V = V_0 + \frac{k_BT}{q_e}\left[\ln\left(\frac{C_{H^+}}{C_{H^+}^0}\right) - \frac{1}{2}\ln\left(\frac{C_{H_2}}{C_{H_2}^0}\right)\right] \tag{S11a}$$

The total mass transport losses of the system are determined by the Nernst potential and "electrostatic potential" V_l at Pt surface

$$\eta_{MT} = V_{l,Pt} + \frac{k_BT}{q_e}\left[\ln\left(\frac{C_{H^+}}{C_{H^+}^0}\right) - \frac{1}{2}\ln\left(\frac{C_{H_2}}{C_{H_2}^0}\right)\right] \tag{S11b}$$

The elementary charge is denoted with q_e, Boltzmann constant with k_B and temperature with T. The concentrations of protons and molecular hydrogen are c_{H+} and c_{H2}, respectively. Superscript 0 denotes the equilibrium concentrations that correspond to the reference potential V_0. Typically the activity of H_2 is approximated with its partial pressure, but it appears that the species that reacts at the electrode is the individual H_2 molecules dissolved in electrolyte, not H_2 in gas bubbles[2,9]. Therefore we use the concentration of dissolved H_2 instead of the partial pressure, when considering electrode kinetics. The equilibrium concentration of H_2 is significantly smaller than the equilibrium concentration of protons, so H_2 concentration will dominate the Nernst potential, as the changes in both concentrations at the electrode surface are quite similar (both due to HER/HOR and mass transport).

Henry's law gives the equilibrium concentration of dissolved gases at low partial pressures, meaning that at low pressures the concentration of dissolved H_2 depends linearly on the pressure of hydrogen outside water.

$$c_{H_2}^0 = \frac{p_{H_2}^0}{k_{H,H_2}} \tag{S12}$$

The literature value of the coefficient $k_{H,H2}$ for H_2 in water at 298.15 K (1282.05 atm/M ≈ 1299.0 bar/M [10]) yields an equilibrium concentration of $c_{H2}{}^0$ = 0.77 mM in 1 bar hydrogen pressure. The coefficient k depends on temperature, but we consider only a single temperature, T^0=298.15K, so the temperature dependence does not affect simulations.

When the effects of bubble formation on the H_2 concentration can be neglected, the concentrations of protons and H_2 on catalyst surface are

$$\frac{C_{H^+}}{C_{H^+}^0} = 1 - \frac{i}{i_{lim,H^+}} \tag{S13a}$$

$$\frac{c_{H_2}}{c_{H_2}^{0}} = 1 - \frac{i}{i_{lim,H_2}} \tag{S13b}$$

Following the convention that for HOR $i>0$ and for HER $i<0$, it follows that $i_{lim,H+}<0$ and $i_{lim,H2}>0$. We simplify the potentials to a dimensionless overpotential η' (which does not include potential V_l for simplicity, unlike overpotential in equation (S5a))

$$\eta' = \frac{q_e(V - V_0)}{k_B T} \tag{S14}$$

Inserting the expressions for the overpotential and surface concentrations into Nernst potential and multiplying both sides by 2 gives

$$2\eta' = 2\ln\left[1 - \frac{i}{i_{lim,H^+}}\right] - \ln\left[1 - \frac{i}{i_{lim,H_2}}\right] = \ln\left[\frac{\left(1 - \frac{i}{i_{lim,H^+}}\right)^2}{1 - \frac{i}{i_{lim,H_2}}}\right] \tag{S15}$$

We then take the exponential of this and reorganize the resulting expression for a quadratic equation of current density

$$\frac{i^2}{i_{lim,H^+}^{2}} + i\left(\frac{e^{2\eta'}}{i_{lim,H_2}} - \frac{2}{i_{lim,H^+}}\right) + 1 - e^{2\eta'} = 0 \tag{S16}$$

Current density is solved by taking the positive root, because it corresponds to $i=0$ when $\eta'=0$.

$$i = \frac{-B + \sqrt{B^2 - 4AC}}{2A} \tag{S17a}$$

$$A = \frac{1}{i_{lim,H^+}^{2}} \tag{S17b}$$

$$B = \frac{e^{2\eta'}}{i_{lim,H_2}} - \frac{2}{i_{lim,H^+}} \tag{S17c}$$

$$C = 1 - e^{2\eta'} \tag{S17d}$$

When the current density is small compared to the limiting current density of HER, i.e. $|i| << |i_{lim,H+}|$ and thus $i/i_{lim,H+} \rightarrow 0$, equation (S16) can be simplified to

$$i \approx i_{lim,H_2}\left(1 - e^{-2\eta'}\right) \tag{S18}$$

Note that this is very similar to the Tafel equation. This shows that, in this case, it is difficult to distinguish a situation where the current – overpotential data is dominated by the mass transport overpotential from a situation where it is dominated by the activation overpotential. In fact, equation (S18) predicts a Tafel-slope of 30 mV/decade Tafel-slope (from the mass transport overpotential). This value for the slope, if produced solely by the activation overpotential, could be possible in the case of the Volmer-Tafel reaction path with a comparably slow Tafel step as the RLS, but not with the other reaction paths dominating. The apparent exchange current density extrapolated from the IV curve then corresponds to the limiting current density of HOR, and *not* the true reaction kinetics[7], a fact which is often not considered [2,6]. In other words, the mass transport overpotential produces an IV-curve that is deceptively similar to a situation with comparatively slow kinetics and Tafel-reaction as the RLS[3,6]. This would explain the seeming discrepancy between very rapid reaction kinetics with Volmer as the RLS measured in high mass transport rate conditions and the numerous cases with much slower reaction kinetics with Tafel as the RLS[3,6].

The mass transport overpotential is illustrated in Figure S1a with limiting current densities calculated for 100 µm diffusion layer thickness with c_{H^+} =1M and c_{H_2} = 0.77 mM (corresponding to p_{H2}=1 bar, diffusion coefficients and mobilities as in **Table 1**).

Proton transport ($i/\, i_{lim,H+}$ in equation (S16)) affects the solution noticeably only, when considering currents that are higher than ~10% of the limiting current density (see Figure S1a, where $i_{lim,H+} \approx 1800$ mA/cm^2). The equilibrium concentration of protons in 1M acid is more than thousand times as high as the concentration of dissolved H_2, and thus $|i_{lim,H+}| >> |i_{lim,H2}|$, because the mobility of protons is also higher than that of H_2 molecules. Therefore H_2 transport dominates mass transport overpotential at all positive and low negative overpotentials.

Figure S1b shows how the mass transport overpotential at 10 mA/cm^2 current density depends on the electrolyte diffusion layer thickness. The typical exchange current density of about 1 mA/cm^2 that can be interpreted as mass transport[3,6] corresponds to about 75 µm diffusion layer thickness, and the typical overpotential of 30 – 40 mV for Pt electrodes used as a benchmark for other catalysts[11] corresponds to about 65 – 160 µm thick diffusion layer (HOR limiting current density 0.47 – 1.17 mA/cm^2). For the simulations we choose to use 100 µm thickness, because it corresponds to overpotential (~34 mV) and limiting current density (~0.76 mA/cm^2) that are roughly at the middle of the aforementioned experimentally observed ranges.

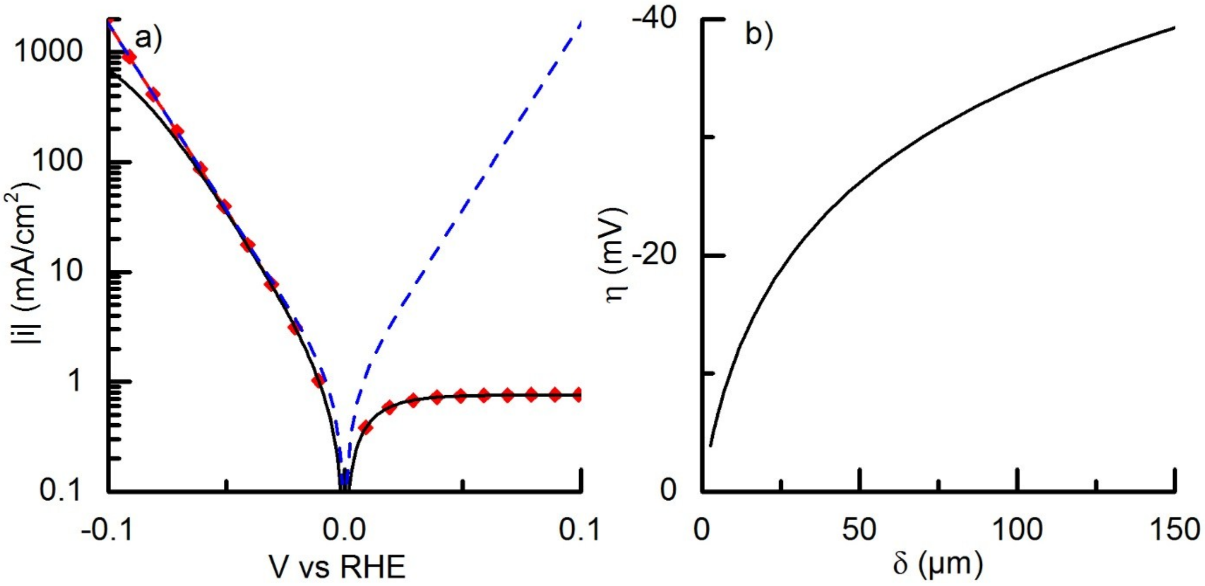

Figure S1 a) The mass transport overpotential assuming a diffusion layer thickness of 100 µm: exact solution (black line, equation (S17)) and the approximate solution (red diamonds, equation (S18)). The dashed blue line is Butler-Volmer equation with $\alpha_a=\alpha_c=2$ (Tafel slope ≈ 30 mA/dec) and $i_0 = i_{lim,H2}$. b) The overpotential required for 10 mA/cm^2 current density as a function of the diffusion layer thickness (exact solution (S17)).

Transport of ions and molecules in liquid

We simulate an aqueous electrolyte with 1M (= mol/l) bulk concentration of perchloric acid ($HClO_4$). In addition to protons and perchlorate ions, molecular hydrogen (H_2) is also dissolved into the liquid and its transport is driven by diffusion. The system is modeled using diffusion domain approach [12,13]. The simulations are calculated in 2D cylindrical geometry with Comsol multiphysics (version 5.0) and the transport in liquid is solved with the Tertiary current distribution mode of Electrochemistry module.

The continuation equation for the species n in the liquid electrolyte is

$$\frac{\partial c_n}{\partial t} = -\nabla \cdot j_n + R_n \tag{S19}$$

The flux of species n is $\boldsymbol{j_n}$ and R_n is its net generation rate. The flux depends on diffusion and electric field, as the liquid was assumed to be stagnant.

$$j_n = -D_n \nabla c_n - z_n \mu_n c_n \nabla V_l = -D_n \left(\nabla c_n - \frac{z_n q_e}{k_B T} c_n \nabla V_l \right) \tag{S20}$$

The concentration of the species in question is c_n, its charge is z_n and D_n and μ_n are its diffusion coefficient and mobility, respectively, and they are connected by Einstein relation ($\mu_n = q_e/k_B T \cdot D_n$). Electroneutrality is enforced everywhere in the electrolyte, meaning that $C_{ClO4-} = C_{H+}$, because they are the only charged species in the system

$$\sum_n z_n c_n = 0 \tag{S21}$$

The gradient of potential V_l (equation (S5a)) corresponds to resistive losses and the different mobilities of protons and perchlorate ions[14]. The overall WE-CE bias is screened by the electrolyte and does not give rise to a net field beyond the outer Helmholtz plane (OHP), and although the potential gradient caused by the mobility difference and resistive losses appears similar to an electric field (***E***=-∇V_l), it corresponds to the effects of coulombic attraction (electroneutrality) on ion transport

$$\nabla V_l = -\frac{k_B T}{q_e}\left[\left(\frac{D_{H^+} - D_{ClO_4^-}}{D_{H^+} + D_{ClO_4^-}}\right)\nabla\left(\ln\frac{c_{H^+}}{c^0_{H^+}}\right) - \frac{i}{q_e N_A c\left(D_{H^+} + D_{ClO_4^-}\right)}\right] \tag{S22}$$

The term $\nabla(\ln(c/c^0))$ is typically marked without c^0 (i.e. as $\nabla(\ln(c))$), as the reference concentration will cancel itself, when the expression is simplified to $(\nabla c)/c$. At the boundary of bulk electrolyte V_l=0 and all concentrations are fixed (i.e. perfect stirring beyond the boundary layer). The flux through the other boundaries is set to be zero.

Although V_l includes ohmic losses in electrolyte, in the studied current density range they were at most 0.6 mV (25 mA/cm^2 and 100 µm diffusion layer thickness, calculated by deducting the concentration dependent component from V_l at Pt surface) and corresponded very accurately to the bulk conductivity of the electrolyte (41.7 S/m based on values in Table 1, comparison not shown). Therefore their inclusion in simulation results has only a negligible effect.

The total current density in the electrolyte is the sum of the ion fluxes

$$i_l = F\sum_n z_n j_n \tag{S23}$$

HER/HOR on Pt is the current source for the mass transport in electrolyte and protons are the only ion that participates in the reaction.

$$\nabla \cdot i_l = F\sum_n z_n R_n \tag{S24}$$

Depending upon whether the species of interest is protons or H$_2$ the reaction will be either a source or a sink

$$R_{H^+,Pt} = \frac{i_V}{q_e N_A} \tag{S25a}$$

$$R_{H_2,Pt} = -v_T = \frac{-i_V}{2q_e N_A} \tag{S25b}$$

The electrode (TiO$_2$ and Pt) is treated as a resistive material with a finite conductivity

$$\nabla \cdot i_s = Q_s \tag{S26a}$$

$$i_s = -\sigma_s \nabla V_s \tag{S26b}$$

HER/HOR is the only current source (Q_s) in the electrode or its boundaries, so Q_s=0 everywhere, except at the exposed Pt surface. At the “bottom” of the TiO$_2$ (z=-100nm) potential V_s is fixed to a set potential (vs RHE in bulk electrolyte), which is the total overpotential that we use (see equation (S5b) and e.g. **Figures 4** and **5**).

Simulation details; Validation of the geometrical considerations

A Pt loading of 10 ng/cm^2 corresponds to a center-to-center distance of about 134 nm and 1000 ng/cm^2 to about 13.4 nm distance (Figure 1). At loadings higher than 1000 ng/cm^2 the average distance between the edges of nearest neighbors is thus less than 8 nm, i.e. comparable to the particle size, meaning that the geometric effects and variations in cluster placement may begin to affect mass transport and therefore the cylindrical approximation may become inaccurate at higher Pt loadings. Depending on the placement geometry of the nanoparticles on the electrode surface, the true average distance between nearest neighbors at a given Pt loading may be smaller than equation (1) predicts, but the difference is not likely significant. For instance, in the case of square array the distance would be about 11% smaller than our approximation.

According to equation **(1)** Pt loading of 7150 ng/cm^2 corresponds to a surface fully covered with the particles (R_{cell}=r_{Pt}), although in reality a lower loading likely suffices for this, because the cylindrical approximation overestimates the average distance. In the simulated geometry the Pt surface area per mass is about 53 m^2/g (or 5.3×10^{-4} cm^2/ng), when the loading is low enough that the particles are separate from each other. With about 1880 ng/cm^2 of Pt the exposed Pt surface area would then be equal to the geometrical area of the electrode, and a smooth 1 nm thick Pt layer contains 2145 ng/cm^2 of Pt.

Results

Characterization of size-selected Pt nanoparticles

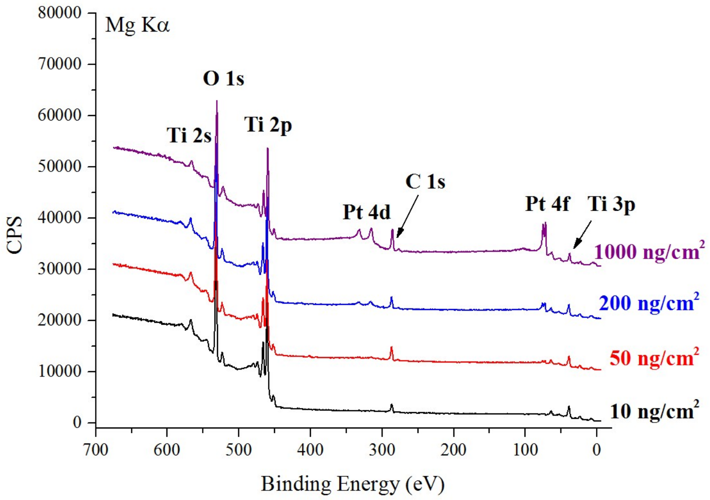

Figure S2. XPS survey spectra measured on the planar photocathodes having different deposited Pt loadings.

The deposited samples were checked with XPS for contaminations. Figure S2 shows representative survey spectra measured on samples previously deposited each of the deposited loadings. No unexpected contaminants were detected on the surface of the samples.

Figure S3 shows overview TEM images of the particles on lacey carbon covered Cu TEM grids. The narrow size-distribution (see Figure 2A) can be seen. The chance of particles landing on top of each other is even less in case of the TiO_2 covered Si samples, as the deposited surface coverage in case of those samples is expected to be less than on the TEM grids, except the highest loading (1000 ng/cm^2) where it is around 3 times higher.

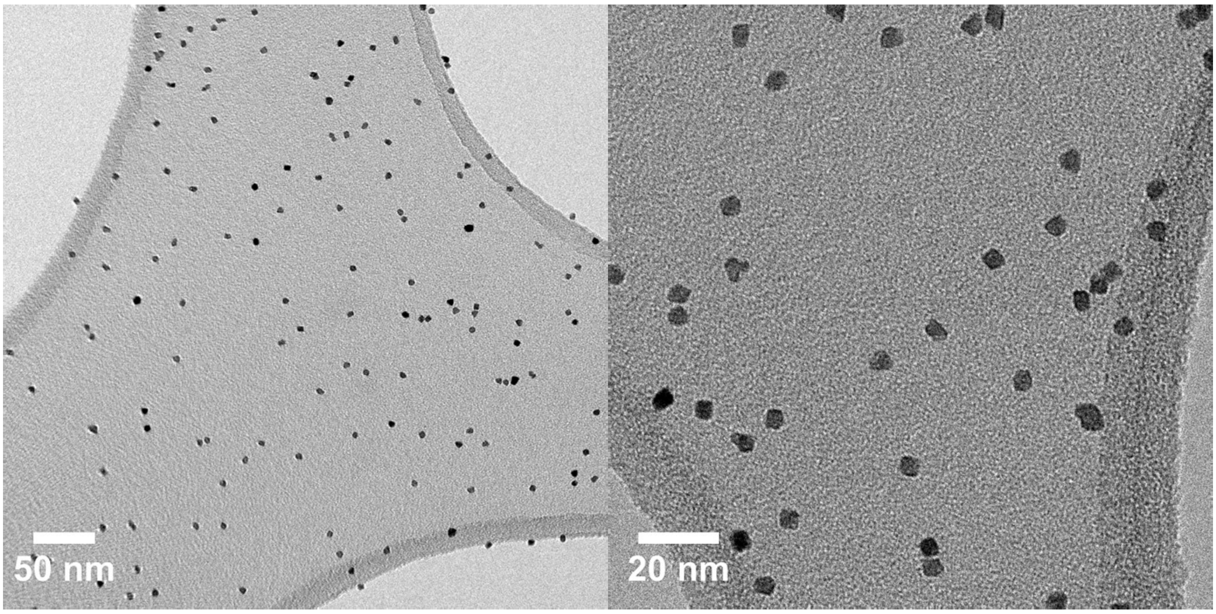

Figure S3. Overview TEM images of the deposited particles.

The effect of exchange rate of Tafel step

The overall effect of increasing or decreasing the exchange rate of Tafel step can be summarized based on equations (S4) – (S6): In steady state the coverage does not change over time, so the reaction rate of Tafel step must corresponds to the current density. Decreasing the exchange rate therefore increases the coverage required to maintain a given HER current density. There are then less free adsorption sites available, leading to higher overpotentials. Ultimately, the highest HER current density that Tafel step allows is limited by the exchange rate and equilibrium coverage

$$i_{T,HER,max} = -\frac{2r_T i_{0,V}}{(\theta^0)^2} \tag{S27}$$

With exchange current density $i_{0,V}$=100 mA/cm^2 and equilibrium coverage θ^0=0.67 [8] the lowest value of r_T that allows the measured current density of about 22 mA/cm^2 with 10 ng/cm^2 loading (about 4.1 A/cm^2 per Pt area) is 9.3. Because initially this was the only criterion for the value of r_T, we analysed, how it affects the overpotential and match with experiments with 10 ng/cm^2.

Figure S4 shows how increasing r_T from 1 to 13 affects the overpotential. At low overpotentials it is difficult to distinguish the IV-curves from each other, but the differences become apparent, when overpotential is increased and values r_T≤9 limit the HER current density to below the measured photocurrent, so they clearly do not correspond to the true kinetics. Based on how r_T values 9.5 and 10 fit the measured curve, it seems that the best fit to experiments corresponds to the HER kinetic limitation being slightly higher than or equal to the photocurrent. We choose to use r_T=9.5, because it approximately corresponds to this limitation (about -4.2 A/cm^2 per Pt area, or with 10 ng/cm^2 loading about -22.5 mA/cm^2 per electrode area).

The choice of the equilibrium coverage and especially Tafel rate are somewhat uncertain and the used values might not correspond to the actual reaction kinetics, especially if in reality Heyrovsky step contributes significantly to current density. Because the best fit to experiments seems to correspond to HER limiting current density being just a little higher than the photocurrent, quite likely several other (θ^0, r_T) combinations that produce the same current density limitation yield an equally good fit. For example, the parameters calculated by Wang et al.[5] (5% equilibrium coverage and 0.043< r_T<0.055) correspond to 18.3 – 23.4 mA/cm^2, and especially r_T=0.055 produces a good fit to measured IV-curve (not shown), but contradicts results that indicate Volmer as the RLS[2,6].

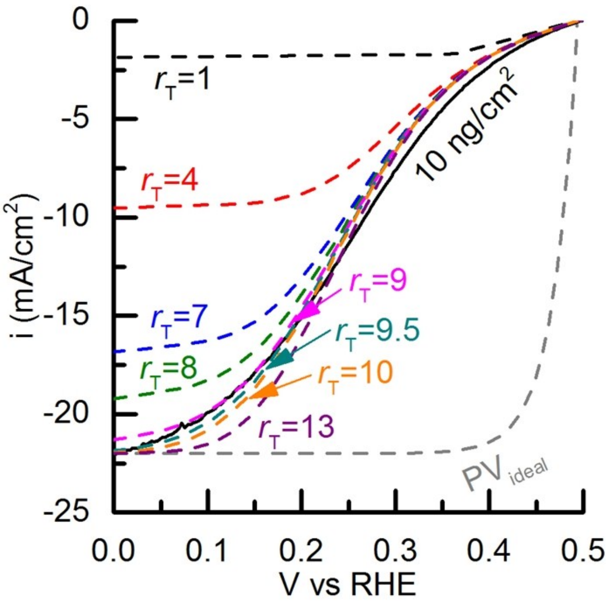

Figure S4 The effect of the exchange rate of Tafel step (r_T) on the HER overpotential with 10 ng/cm^2 Pt loading.

The Effect of mass transport rate on the total overpotential

As explained before, we initially chose 100 µm diffusion layer thickness for the simulations. With 0.77 mM H_2 concentration this corresponds to HOR limiting current density of about 0.76 mA/cm^2. This led to overestimated overpotentials at low current densities with the highest loadings (200 ng/cm^2 and 1000 ng/cm^2). When the total overpotential was plotted similarly to **Figure 5** (not shown), the results indicated that at high loadings (and especially at current densities less than 20 mA/cm^2) the total overpotential η_{total} was almost equal to the mass transport overpotential η_{MT}. To determine what diffusion layer thickness would match the experimental results we analysed its effects on the total overpotential with 1000 ng/cm^2 loading that was the most sensitive to mass transport conditions due to the lowest kinetic losses.

Figure S5 below shows the simulated overpotentials for diffusion layer thicknesses ranging from 2.5 µm (30.4 mA/cm^2) to 100 µm (0.76 mA/cm^2). Overall, 5.0 µm thickness (15.2 mA/cm^2) seems to be the best match to the measured IV curve, although all thicknesses from 2.5 µm to 10.0 µm (7.6 mA/cm^2) are close to measured IV curve and more detailed analysis could yield slightly different diffusion layer thickness and a bit better fit to measured IV-curve. However, the difference between 2.5 µm and 5.0 µm thicknesses at 20 mA/cm^2 current density is about 5 mV (which is also the difference between 5.0 µm and 10.0 µm), so further optimization will not significantly improve the fit. The assumptions and inaccuracies associated with the IV curve of the ideal PV cell could well correspond to a larger error than the aforementioned 5 mV difference. Therefore the actual mass transport rate cannot be determined accurately, but is likely in the range of about 7.5 - 30 mA/cm^2 HOR limiting current density. Overall, explaining the low overpotentials with 1000 ng/cm^2 requires very high mass transport rates: even 7.6 mA/cm^2 limiting current density (10 µm diffusion layer thickness) is so high that under 1 bar H_2 pressure it may be impossible to achieve even with a RDE, so these conditions seem unlikely in stirred electrolyte.

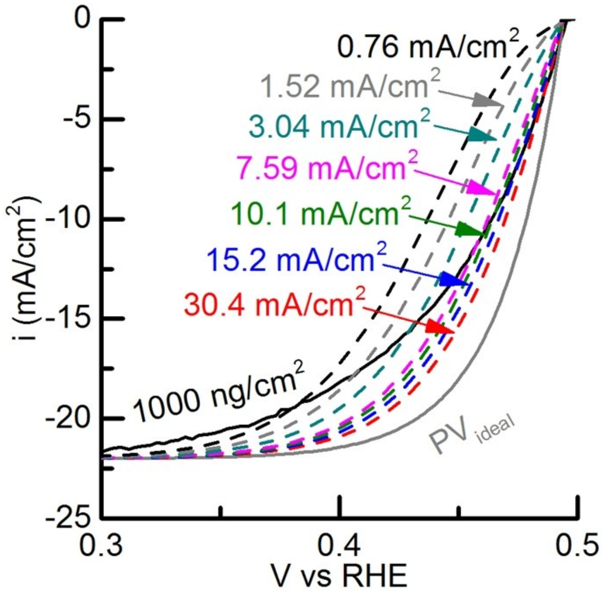

Figure S5 The simulated overpotentials (dashed lines) for 1000 ng/cm² with HOR limiting current densities ranging from 0.76 mA/cm² (100 µm thick diffusion layer) to about 30.4 mA/cm² (2.5 µm) compared to measured IV-curve (solid black line).

The measured IV-curve being explained by very high mass transport rate is most likely related to the potential sweep, because the measurements and simulations correspond to different situations in the sense that the measurements are carried out as a CV potential sweep, whereas the simulations were calculated until steady state was achieved. High sweep rate probes mass transport only comparatively close to the electrode surface, and thus the mass transport losses may correspond to a relatively thin diffusion layer (compared to the steady-state characteristics of simulations).

Importantly to HER on Pt, the sweep rates and exchange current densities with ~30 mV/decade Tafel-slope in literature seem to correlate with each other, with lowest sweep rates yielding lowest exchange current densities (see **Figure S6**).[15–20] In all the referred cases the aim was to measure the steady state operation of the studied catalysts and Pt electrode, so they are representative of typical measurement methods and their biases. The sample size of five studies is not very large, so the result could be a coincidence and a larger literature review and/or experimental study would be required to assess the situation more accurately. However, the exact determination of the effect of the sweep rate is beyond the scope of this article.

Despite **Figure S6** suggesting that our scanning rate (50 mV/s) is unusually high compared to literature, this is not the case. Scanning rates up to at least 40 mV/s[21] have been used, but our analysis is limited to cases, where information about mass transport conditions was readily available. This likely creates a bias to comparatively low sweep rates, because, as **Figure S6** suggests, mass transport losses could be too small to notice or determine accurately with sweep rates much higher than 10 mV/s.

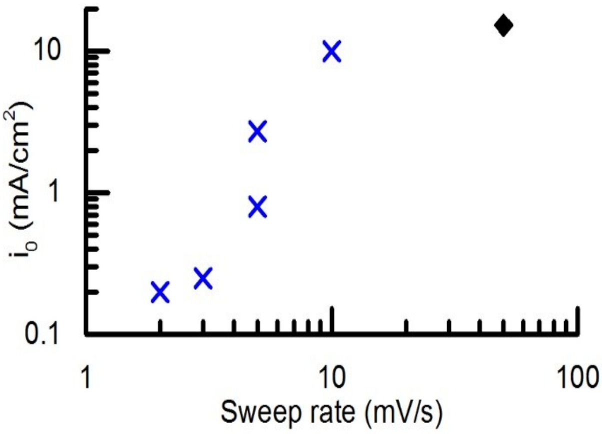

Figure S6 Literature data about HOR limiting current density/apparent HER exchange current density as a function of the sweep rate. This article is marked with black diamond.

Effect of exchange current density on HER overpotential

As **Figure 5** shows, the overpotential of 10 ng/cm^2 loading reflects the reaction kinetics most accurately. Therefore we used it study the effect of exchange current of Volmer step (i_{0V}) on the simulated overpotential. Because we already established that the best fit to experiments appears to correspond to the kinetic limit of HER being approximately equal to the photocurrent with 10 ng/cm^2, we also vary the value of r_T with the exchange current density to match this criterion, i.e. $r_T \times i_{0V}$ =950 mA/cm^2. In accordance with the mass transport analysis, we use diffusion layer thickness 5 µm as a difference to **Figure S4**.

The effect of exchange current density is illustrated in **Figure S7** below. Reducing it from 100 mA/cm^2 to 90 mA/cm^2 could improve the match a little, but not significantly, so we continue to use 100 mA/cm^2 (and r_T = 9.5).

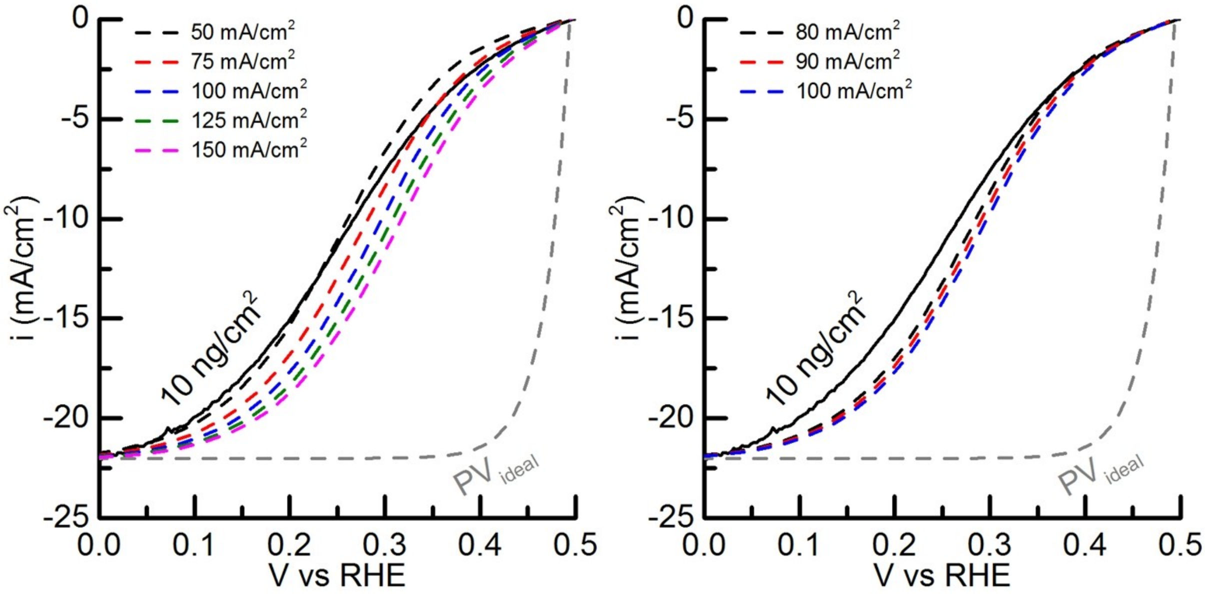

Figure S7 The effect of exchange current density on HER overpotential with 10 ng/cm^2 Pt loading. Solid black line corresponds to measured IV-curve and grey to ideal PV (*n=1*)

The effect of particle size on overpotentials

In Figure S8 the effect of particle size is illustrated with three different sizes (d=2nm, 5nm and 10nm, different markers) and two current densities (10 and 20 mA/cm^2, color of the markers). As shown in Figure 5 in the main text, mass transport losses are almost same for all loadings, so the differences in overpotentials are due to reaction kinetics: Smaller particles have more surface area per mass and so, for a given loading and current density per electrode area, the current density per Pt surface area is smaller. Consequently, the overpotential is reduced. With the selected particle sizes there are clear differences, and the overpotential with 2 nm particles at 20 mA/cm^2 is approximately equal to the overpotential for 10 mA/cm^2 with 5 nm particles. Similarly, the overpotential for 5 nm particles and 20 mA/cm^2 current density is approximately equal to the overpotential with 10 nm particles at 10 mA/cm^2 current density. This suggests that Pt consumption could be reduced and the electrode performance improved from our experimental results with smaller particles, if the reduced size does not cause problems.

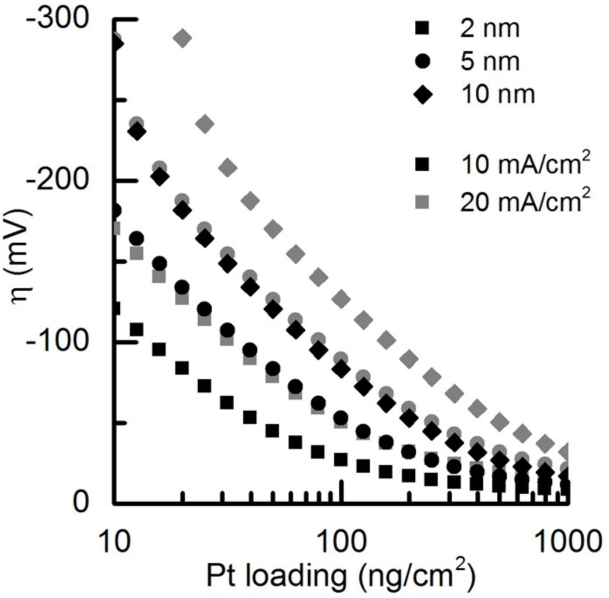

Figure S8 The effect of particle size on the overpotential for different Pt loadings.

References

1 J. Durst, A. Siebel, C. Simon, F. Hasché, J. Herranz and H. A. Gasteiger, *Energy Environ. Sci.*, 2014, **7**, 2255–2260.

2 P. J. Rheinländer, J. Herranz, J. Durst and H. A. Gasteiger, *J. Electrochem. Soc.*, 2014, **161**, F1448–F1457.

3 K. C. Neyerlin, W. Gu, J. Jorne and H. A. Gasteiger, *J. Electrochem. Soc.*, 2007, **154**, B631–B635.

4 S. Chen and A. R. Kucernak, *J. Phys. Chem. B*, 2004, **108**, 13984–13994.

5 J. X. Wang, T. E. Springer and R. R. Adzic, *J. Electrochem. Soc.*, 2006, **153**, A1732–A1740.

6 J. Durst, C. Simon and H. A. Gasteiger, *J. Electrochem. Soc.*, 2015, **162**, F190–F203.

7 J. Harrison and Z. Khan, *J. Electroanal. Chem. Interfacial Electrochem.*, 1971, **30**, 327–330.

8 N. M. Markovic and P. N. J. Ross, *Surf. Sci. Rep.*, 2002, **45**, 117–229.

9 K. Aoki, H. Toda, J. Yamamoto, J. Chen and T. Nishiumi, *J. Electroanal. Chem.*, 2012, **668**, 83–89.

10 D. R. Lide, Ed., *CRC Handbook of Chemistry and Physics*, CRC Press, 95th edn., 2014.

11 P. C. K. Vesborg, B. Seger and I. Chorkendorff, *J. Phys. Chem. Lett.*, 2015, 951–957.

12 H. Reller, E. Kirowa-Eisner and E. Gileadi, *J. Electroanal. Chem. Interfacial Electrochem.*, 1982, **138**, 65–77.

13 R. G. Compton, G. G. Wildgoose, N. V. Rees, I. Streeter and R. Baron, *Chem. Phys. Lett.*, 2008, **459**, 1–17.

14 J. A. Manzanares and K. Kontturi, in *Encyclopedia of Electrochemistry, Volume 2, Interfacial Kinetics and Mass Transport*, 2003, pp. 81–145.

15 Y. Li, H. Wang, L. Xie, Y. Liang, G. Hong and H. Dai, *J. Am. Chem. Soc.*, 2011, **133**, 7296–7299.

16 M. S. Faber, R. Dziedzic, M. A. Lukowski, N. S. Kaiser, Q. Ding and S. Jin, *J. Am. Chem. Soc.*, 2014, **136**, 10053–10061.

17 J. Xie, H. Zhang, S. Li, R. Wang, X. Sun, M. Zhou, J. Zhou, X. W. Lou and Y. Xie, *Adv. Mater.*, 2013, **25**, 5807–5813.

18 E. J. Popczun, J. R. McKone, C. G. Read, A. J. Biacchi, A. M. Wiltrout, N. S. Lewis and R. E. Schaak, *J. Am. Chem. Soc.*, 2013, **135**, 9267–9270.

19 J. Kibsgaard and T. F. Jaramillo, *Angew. Chemie Int. Ed.*, 2014, **53**, 14433–14437.

20 H. A. Gasteiger, S. S. Kocha, B. Sompalli and F. T. Wagner, *Appl. Catal. B Environ.*, 2005, **56**, 9–35.

21 Y. Chen, K. Sun, H. Audesirk, C. Xiang and N. Lewis, *Energy Environ. Sci.*, 2015.